THE JOURNAL OF BIOLOGICAL CHEMISTRY
Vol. 278, No. 15, Issue of April 11, pp. 13216–13226, 2003
Printed in U.S.A.

Mot1 Regulates the DNA Binding Activity of Free TATA-binding Protein in an ATP-dependent Manner*

Received for publication, November 10, 2002, and in revised form, January 10, 2003
Published, JBC Papers in Press, February 4, 2003, DOI 10.1074/jbc.M211445200

Russell P. Darst‡, Arindam Dasgupta‡, Chunming Zhu, Jer-Yuan Hsu§, Amy Vroom, Tamara Muldrow, and David T. Auble¶

From the Department of Biochemistry and Molecular Genetics, University of Virginia, Charlottesville, Virginia 22908

Mot1 is an essential Snf2/Swi2-related *Saccharomyces cerevisiae* protein that binds the TATA-binding protein (TBP) and removes TBP from DNA using ATP hydrolysis. Mot1 functions *in vivo* both as a repressor and as an activator of transcription. Mot1 catalysis of TBP·DNA disruption is consistent with its function as a repressor, but the Mot1 mechanism of activation is unknown. To better understand the physiologic role of Mot1 and its enzymatic mechanism, *MOT1* mutants were generated and tested for activity *in vitro* and *in vivo*. The results demonstrate a close correlation between the TBP·DNA disruption activity of Mot1 and its essential *in vivo* function. Previous results demonstrated a large overlap in the gene sets controlled by Mot1 and NC2. Mot1 and NC2 can co-occupy TBP·DNA *in vitro*, and NC2 binding does not impair Mot1-catalyzed disruption of the complex. Residues on the DNA-binding surface of TBP are important for Mot1 binding and the Mot1·TBP binary complex binds very poorly to DNA and does not dissociate in the presence of ATP. However, the binary complex binds DNA well in the presence of the transition state analog ADP-AlF$_4$. A model for Mot1 action is proposed in which ATP hydrolysis causes the Mot1 N terminus to displace the TATA box, leading to ejection of Mot1 and TBP from DNA.

A critical step in the assembly of an active transcription complex at an RNA polymerase II promoter involves recruitment of TATA-binding protein (TBP)[1] and TBP-associated factors (1–3). TBP recruitment and activity are influenced by a large number of transcription factors and components of the general transcription machinery, many of which can interact directly with TBP (3–6). *MOT1* was uncovered in genetic screens for factors that repress transcription driven by a weak promoter (7–11). Consistent with its function as a repressor, Mot1 was isolated independently as an ATP-dependent factor that disrupts the TBP·DNA complex (12). Mot1 binds the TBP·DNA complex *in vitro* (12) and contacts both TBP and about 17 bp of DNA upstream of the TATA box (13). In the absence of DNA, Mot1 also dimerizes with TBP (13–15). In this report, we refer to the Mot1·TBP complex as the "binary" complex, and the Mot1·TBP·DNA complex is referred to as the "ternary" complex.

Mot1 homologs have been identified in many eukaryotes. The human homolog is BTAF1, which interacts with TBP (16, 17) and catalyzes disruption of human TBP·DNA complexes (17). The insect homolog, the 89B helicase (18), may interact with TBP or TBP-related factor 1 (TRF1) *in vitro* (19). The Mot1 C terminus contains the conserved ATPase domain (7), whereas the Mot1 N terminus is responsible for TBP binding (19–21). The structural basis for Mot1·TBP recognition is unknown, however, it was recently suggested that the Mot1 N terminus contains HEAT or ARM repeats, which compose a class of structurally related leucine-rich repeats (22–24). Structural studies have shown that HEAT and ARM repeats form two α helices joined by a short loop (ARM repeats have a short additional α helix), and these can stack upon each other to form a "superhelix" that provides an extensive surface for macromolecular interaction (22). Previous analysis of Mot1 deletion mutants indicated that an extended portion of the Mot1 N terminus is responsible for recognition of TBP (19, 20). It has also been reported that, in solution, Mot1 is a non-globular monomer (15). Taken together, these data suggest a model in which Mot1 adopts an extended conformation that provides a large surface for interaction with TBP. To test the model, mutations were made in both Mot1 and TBP, and the effects on the Mot1·TBP interaction were determined. Because HEAT and ARM repeats are based mostly on hydrophobic interactions (22), it was expected that most polar residues in the N-terminal domain would not be essential, which we have found to be the case.

Mot1 is a member of the Snf2/Swi2 ATPase family (25–27). It has been suggested that at least some Snf2/Swi2 ATPases are processive molecular motors, acting by driving DNA translocation or rotation (28, 29). The Mot1·TBP·DNA system has been used to test several theories about how these ATPases drive changes in protein·DNA interactions. Mot1 is not a helicase (13–15), nor does it travel long distances on DNA after TBP is removed from the TATA box (30). Catalysis of TBP·DNA disruption requires a grip by Mot1 on both upstream DNA and TBP, although the upstream DNA and the TBP·DNA complex can be conformationally uncoupled without impairing catalysis (13). These results indicate that Mot1 does not dissociate TBP·DNA by propagation of DNA twist or writhe through the TATA box. A similar result has been reported for the Snf2/Swi2 family member ISWI (31). It is possible that Mot1 interacts with the TATA box directly and in so doing alters its structure or that Mot1 uses ATP hydrolysis to disrupt TBP·DNA complexes via short-range tracking or ATP-driven insertion of

* This work was supported by National Institutes of Health Grant GM55763 (to D. T. A.). The costs of publication of this article were defrayed in part by the payment of page charges. This article must therefore be hereby marked "*advertisement*" in accordance with 18 U.S.C. Section 1734 solely to indicate this fact.

‡ Both authors contributed equally to this work.

§ Present address: Division of Biology, University of California at San Diego, 9500 Gilman Dr., La Jolla, CA 92093.

¶ To whom correspondence should be addressed: Dept. of Biochemistry and Molecular Genetics, University of Virginia Health System, 1300 Jefferson Park Ave., Charlottesville, VA 22908-0733. Tel.: 434-243-2629; Fax: 434-924-5069; E-mail: dta4n@virginia.edu.

[1] The abbreviations used are: TBP, TATA-binding protein; ORF, open reading frame; ts, temperature-sensitive; GST, glutathione *S*-transferase; ARM, armadillo.

Mot1 into the TBP·DNA interface. Alternatively, Mot1 may mediate TBP·DNA disruption by inducing a conformational change in TBP that deforms the DNA-binding surface of TBP. Here we demonstrate that residues on the DNA-binding surface of TBP impair the interaction of TBP with Mot1, suggesting that Mot1 contacts the DNA-binding surface of TBP, and explaining why the Mot1·TBP binary complex binds DNA poorly compared with TBP alone. Binding of an ATP transition state analog locks the binary complex into a form in which the Mot1·TBP complex can bind DNA better than the nucleotide-free form of the Mot1·TBP complex. These results suggest that ATP hydrolysis causes a change in either the conformation of TBP or the interaction of Mot1 with the DNA-binding surface of TBP and that these ATP-driven conformational changes explain how Mot1 drives disruption of the TBP·DNA complex.

MATERIALS AND METHODS

mot1 Library Construction and Screening—Oligonucleotide primers flanking the *Eco*RI site (bp position 1026 in the *MOT1* open reading frame (ORF)) and *Cla*I site (position 2092) were used to amplify ~1 kb of the *MOT1* ORF using *Taq* polymerase under reduced fidelity conditions as described previously (32). The PCR-amplified DNA was digested with *Eco*RI and *Cla*I and cloned into an *Eco*RI-*Cla*I-gapped plasmid containing the rest of the *MOT1* ORF under control of the *GAL1* promoter on a *CEN ARS* plasmid bearing the *LEU2* gene (20). Note that an additional *Cla*I site is present in the *MOT1* ORF, but this second site is blocked from *Cla*I digestion by overlapping *dam* methylation. Six independent transformants were picked at random from the bacterial transformation of the primary ligation mix, and these were sequenced and found to contain ~1-bp change per kilobase (kb) of amplified DNA. Bacterial transformants containing the mutated DNA were then scraped *en masse* from agar plates, inoculated at high density into liquid media, and used in a large-scale plasmid purification prep. The resulting purified plasmids were then used to transform yeast strain AY29 (*mot1*Δ::*TRP1*, carrying plasmid pMR13 (*MOT1*+ *URA3*+)) (20), which is otherwise congenic to YPH499 (33) by selection on synthetic complete media containing glucose but without leucine using standard techniques (34). Approximately 13,000 transformants were replica-plated to synthetic glucose- or galactose-containing media lacking leucine and incubated at 30 °C for 3–5 days. Comparison of the glucose and galactose-containing plates did not reveal any *GAL1*-inducible alleles of *MOT1*, which caused slow growth in the presence of wild-type *MOT1*. Colonies were then replica-plated from galactose-containing media to media containing galactose and 5-fluoroorotic acid (34) to select for loss of the *URA3*-marked plasmid containing the wild-type *MOT1* gene. Approximately half of the transformants did not survive the 5-fluoroorotic acid selection, indicating that these strains harbored alleles of *MOT1*, which do not support growth in the absence of wild-type *MOT1*. The remaining viable strains were screened for temperature-sensitive growth defects by replica plating to synthetic galactose plates minus leucine and incubation at 30 °C and 35 °C. Temperature-sensitive strains were re-streaked, and the plasmids were isolated and re-transformed to the *MOT1* deletion strain to confirm the plasmid-linked temperature-sensitive (ts) phenotype. Candidate genes were then sequenced through the entire *Eco*RI-*Cla*I region of the ORF, and the mutant fragments were subcloned to a new plasmid backbone containing the remainder of the *MOT1* gene to be sure that mutations in the *Eco*RI-*Cla*I DNA fragment were responsible for the phenotypes observed.

Site-directed MOT1 Mutants—Site-directed mutagenesis was performed using synthetic oligonucleotides and either overlapping PCR or the Stratagene QuikChange kit, according to the instructions provided by the manufacturer. Each mutation was engineered to encode a change in a restriction site (either introduction of a new site or loss of an existing site) to facilitate subcloning. Candidate transformants containing the correct restriction sites were then sequenced completely in a region that overlaps a DNA fragment with convenient restriction sites. The sequenced DNA fragment was then sub-cloned to *LEU2 CEN ARS* plasmids derived from pRS315 (33) that contain the *MOT1* ORF driven by the *GAL1* promoter or by a 448-bp fragment of the *MOT1* promoter. All constructs encode a Mot1 derivative with the Py tag (35) appended to the N terminus to facilitate quantitation by Western blotting and purification using antibody-coupled beads (20, 35). Additional details regarding plasmid construction are available upon request. Plasmids containing the site-directed alleles were transformed into AY29 yeast cells (see above), and the ability of the constructs to support viability was assessed by plasmid shuffling using standard techniques (34). Strains harboring alleles under control of the *MOT1* promoter were analyzed for growth defects on synthetic media without leucine and containing raffinose, galactose, or glucose as the carbon source. Strains harboring alleles under control of the *GAL1* promoter were streaked to galactose-containing plates to induce expression prior to plasmid shuffling. Growth of strains was compared with congenic wild-type cells by incubation at 16 °C, 30 °C, 32 °C, and 35 °C.

Purification of Recombinant TBP and TBP Mutants—Recombinant full-length TBP and TBP mutants expressed under the control of the T7 promoter as a fusion with N-terminal six-histidine tag were obtained by transformation of BL21(DE3) *Escherichia coli* cells with the appropriate plasmid expression vectors (13, 36). Cells were inoculated into 1 liter of yeast extract Tryptone (YT) media containing 100 μg/ml ampicillin or 30 μg/ml kanamycin at 37 °C and were grown to an optical density at 600 nm of 0.7–1.0. Isopropyl-β-D-thiogalactopyranoside was added (0.5 mM final concentration), and the cells were incubated at 37 °C for 3 h to allow protein expression. Cells were harvested and resuspended in buffer I (40 mM sodium phosphate, pH 8.0, 300 mM NaCl, 10% glycerol, 1 mM phenylmethylsulfonyl fluoride, 2 μM benzamidine, 2 μM pepstatin, 0.6 μM leupeptin, and 2 μg/ml chymostatin) containing 5 mM imidazole and lysed by sonication. After sonication, the cleared lysate was incubated at 4 °C for 1 h with 0.2 ml of nickel-nitrilotriacetic acid-agarose (Qiagen) pre-equilibrated with buffer I, which included 5 mM imidazole. The mixture was then loaded into a column, and the resin was washed with 10 ml buffer I plus 5 mM imidazole and subsequently with 5 ml of buffer I containing 20 mM imidazole. Finally, the bound protein was eluted with buffer I containing 200 mM imidazole. The yield was quantitated by Bradford assay (Bio-Rad), and the purity was assessed by Coomassie Blue staining of 10% protein gels. Based on the Coomassie Blue staining, the proteins were estimated to be about 90% pure.

Native Gel Electrophoresis—For detection of TBP by native gel electrophoresis (Figs. 6*C*, 6*D*, and 7*B*), full-length TBP and Mot1 were incubated in binding buffer (13) containing 120 mM KCl and 12 mM HEPES buffer, pH 7.6 (37), using proteins at the concentrations indicated in figure legends. The gels in Figs. 6*C* and 7*B* were run with the electrodes reversed: samples were loaded on the side of the positive electrode, and run toward the negative electrode. The gel was, however, pre-run for >50 min with the electrodes connected in the usual fashion before loading. Following electrophoresis, the gels were boiled in 1% SDS for 1 min, then transferred to Immobilon and TBP was detected using TBP antiserum. The TBE gel shift assay in Fig. 8*A* was performed as described previously (38). Gel shift assays were otherwise performed as described previously (13) using 5 nM core domain TBP (gift of J. Geiger) or full-length TBP with minor modifications as indicated. Synthesis and labeling of the 36- and 17-bp DNAs, and preparation of the radiolabeled 100-bp adenovirus major late promoter fragment, was as previously described (13). DNA concentration was about 0.5 nM in the reactions. The concentration of Mot1 needed to bind 50% of the TBP·DNA complex is ~5 nM (13). The concentration of Mot1 used was estimated from this activity and is indicated in the figure legends. ATP was used at between 5 and 100 μM. ADP was used at 100 μM. NaF was used at 2.5 mM. $AlCl_3$ was used at 10 μM (39). Bur6 was used at 13 nM and Ydr1/Ncb2 at 60 nM (38); both proteins were a gift of G. Prelich.

Purification of Mot1 and Pull-down Assays—Mot1 was expressed and purified from yeast using antibody-coupled beads exactly as described previously (20). The antibody-coupled beads were prepared using Py monoclonal antibody that recognizes the Mot1 epitope tag (20), which was prepared at the University of Virginia Lymphocyte Culture Center. For detection of TBP binding to immobilized Mot1, Mot1-coupled beads were equilibrated with buffer T-60 (30 mM Tris (pH 8.0), 5 mM magnesium chloride, 0.1% Brij-58, 1 mM dithiothreitol, protease inhibitors plus 60 mM potassium chloride). One hundred nanograms of full-length recombinant yeast TBP (or TBP mutant) was added in 500 μl of buffer T-60, and the reaction was incubated for 30 min at room temperature. After binding, the unbound material was collected and the beads were washed with buffer T containing increasing concentrations of KCl; samples marked "Eluate" were collected in T-1000. The eluted proteins were precipitated with acetone, and TBP present in the eluates was detected by Western blotting using rabbit polyclonal anti-TBP antisera.

Preparation of GST-TBP and Mot1 Binding to GST-TBP—One-liter cultures of DH10B bacterial cells containing plasmid pGEX-1 (Amersham Biosciences) or a plasmid expressing GST fused to full-length yeast TBP (kindly provided by Ron Reeder) were grown in YT medium at 37 °C to an optical density at 600 nm of 0.7–1.0. Isopropyl-β-D-

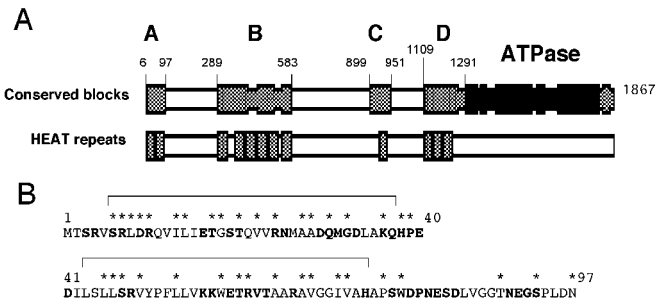

FIG. 1. **Conserved sequence motifs in Mot1.** *A*, the *top schematic* shows the position of conserved blocks in the Mot1 amino acid sequence identified by comparing Mot1 homologs using the programs ClustalW and MACAW (see "Materials and Methods"). Conserved Mot1 blocks are designated *A*, *B*, *C*, and *D*, and the conserved Snf2/Swi2-like ATPase is *shaded black*. *Numbers* indicate boundaries of the conserved regions in *S. cerevisiae* Mot1. Note that these programs identified three conserved blocks of sequence connected by short linker sequences in the region spanning residues 289–583, and the entire region is referred to as the *B block*. The *bottom schematic* shows the positions of HEAT repeats in *gray* (23, 24). *B*, sequence of the Mot1 A block. *Brackets* indicate the positions of the two hydrophobic HEAT repeats. Residues mutated in this study appear in *boldface*, and *asterisks* mark residues identical in yeast Mot1 and human BTAF1. Yeast Mot1 and human BTAF1 are 40% identical over the A block.

thiogalactopyranoside was added (1.0 mM, final concentration), and the cells were incubated at 37 °C for an additional 3 h. Cells were harvested by centrifugation and resuspended in 20 ml of buffer T (30 mM Tris-HCl, pH 8.0, 2 μM pepstatin A, 1 mM phenylmethylsulfonyl fluoride) containing 150 mM KCl (T-150 buffer). Cells were lysed by sonication, and debris was removed by centrifugation. After centrifugation, 0.5 ml of GST lysate or 1.5 ml of GST-TBP lysate was incubated at 4 °C for 1 h with 20 μl of glutathione-agarose equilibrated with buffer T containing 60 mM KCl (T-60). The agarose was washed three times with 1 ml of T-150 buffer, and the entire 20-μl sample of agarose-bound material was used for testing the binding of Mot1. 10 ng of the eluted Mot1 protein obtained from yeast overexpression strains (see above) was added to a 20-μl suspension of GST or GST-TBP agarose in T-60 buffer and incubated on a roller for 1 h at 4 °C. The agarose was washed once with 0.6 ml of T-60 buffer, then an elution step was carried out with 0.6 ml of T-60 buffer with 5 mM $MgCl_2$, with or without 50 μM ATP and with or without 1 nM TATA sequence DNA. Eluted proteins were precipitated with acetone for analysis by Western blotting using the Py antibody (35), which recognizes the N-terminal epitope tag.

Sequence Analysis—Blocks of conserved sequences in the Mot1 N terminus were identified with a set of Mot1 homologs found in Entrez protein sequence data bank (available at www.ncbi.nlm.nih.gov/entrez/query.fcgi?db=Protein) (from *Homo sapiens* (accession number AAC04573), *Arabidopsis thaliana* (T47857), *Saccharomyces cerevisiae* (P32333), *Schizosaccharomyces pombe* (T40642), and *Drosophila melanogaster* (AAF55260)) using the MACAW (40) and ClustalW algorithms (available at www.ibc.wustl.edu/service/msa/index.html). HEAT repeats in Mot1 reported by previous authors (23, 24) included five in the B block. We observed sequence similarity of the second B block HEAT repeat to sequences immediately downstream using MACAW. This had not been found in the original sequence analysis, and Fig. 1*B* therefore includes an additional HEAT repeat in the B block, for a total of six.

RESULTS

Four Conserved Regions in Mot1 N Terminus—Alignment of Mot1 homologs revealed conserved blocks outside of the ATPase, which we designate A–D (Fig. 1*A*). These blocks were not found in any protein except Mot1 or its homologs. The A and B blocks in the human and yeast proteins are about 40% identical. For example, Fig. 1*B* shows the sequence of the *S. cerevisiae* Mot1 A block; the *asterisks* indicate residues that are identical in the yeast and human proteins. Mot1 contains a series of HEAT repeat sequences dispersed throughout the N terminus (23, 24). Remarkably, the four conserved N-terminal domains of Mot1 coincide with the positions of the HEAT repeats (Fig. 1, *A* and *B*; the *brackets* in Fig. 1*B* indicate where two HEAT repeats fall within the A block).

Temperature-sensitive Alleles of mot1—PCR-based mutagenesis was used to introduce random changes in the *MOT1* open reading frame in the region between codons for Arg-345 and Asn-697. This region was chosen because previous deletion analysis indicated an important role for residues in this region in TBP recognition (19, 20). A *CEN ARS* plasmid library expressing mutagenized *mot1* under *GAL1* control was used, because genes that express catalytically defective mot1 were expected to be dominant inhibitors of cell growth (20). Library construction and screening are described under "Materials and Methods." Note that 35 °C was chosen for the non-permissive temperature, because the wild-type *MOT1+* strain used in these studies is itself somewhat growth-impaired at temperatures above 35 °C (not shown). The alleles isolated are recessive, and most of these contain multiple base pair changes (Table I). A single amino acid change, L383P, is responsible for the temperature-sensitive (ts) growth phenotype of a strain harboring *mot1-41*, because the same mutation in *mot1-42* conferred the same phenotype. However, more than one amino acid change is required for the ts phenotypes conferred by *mot1-71* and *mot1-81*, because no single amino acid change encoded by these alleles resulted in the conditional phenotype; several pairwise combinations of mutations in conserved residues also failed to confer a ts phenotype (not shown). The *mot1-14* phenotype likely results from a low level of translational by-pass of the premature stop codon substituted for Trp-496, because deletion of the *mot1* open reading frame downstream of this stop codon is lethal (not shown).

Growth phenotypes of strains carrying the *GAL1*-driven alleles are summarized in Table I. Comparison of strain growth by serial dilution spot assay demonstrated that, compared with wild-type cells, the *mot1* strains displayed growth defects of ~100–1000-fold when incubated at 35 °C (not shown). Growth phenotypes of these *mot1* strains were similar regardless of whether the alleles were expressed under control of the *GAL1* or *MOT1* promoters. Western blot analysis of whole cell extracts from cells grown at 30 °C, using an antibody that recognizes epitope-tagged versions of these proteins, demonstrated that proteins encoded by *mot1-41*, *mot1-71*, and *mot1-81* were expressed at wild-type levels, whereas full-length protein encoded by *mot1-14* was nearly undetectable (Fig. 2*A*). Mot1 protein level in the *mot1-42* strain is intermediate (Fig. 2*A*, *lane 8*).

Wild-type and mutant Mot1 proteins were purified from yeast overexpression strains using antibody-coupled beads (20). The purified proteins were then tested in gel mobility shift assays for the ability to bind TBP·DNA complexes and for ATP-dependent TBP·DNA disruption activity (20). As shown in Fig. 2*B* (*lanes 1–7*), addition of wild-type Mot1 led to formation of Mot1·TBP·DNA ternary complexes that were disrupted in the presence of ATP. The Mot1-41, Mot1-42, Mot1-71, and Mot1-81 proteins did not stably bind to TBP·DNA complexes. These proteins also failed to disrupt TBP·DNA complexes in the presence of ATP even when severalfold more protein was used than was required for wild-type Mot1 to quantitatively supershift and disrupt the TBP·DNA complexes formed under these conditions (Fig. 2*B*, *lanes 8–13*, and Fig. 2*C*). Thus, the defects in cell growth resulting from Mot1-41, Mot1-42, Mot1-71, or Mot1-81 can be explained by general defects of these proteins in TBP·DNA recognition.

Alanine Scanning Mutations in the MOT1 A Block—To map the surface of Mot1 required for TBP binding, extensive mutagenesis of the N-terminal conserved regions was undertaken. While this work was in progress, it was reported that the A and B blocks contain HEAT (or ARM) repeats (22–24). These repeats stack via hydrophobic interactions to form an extended,

TABLE I
Growth of strains harboring temperature-sensitive alleles of mot1 under GAL1 control

Allele	Growth[a]		Amino acid changes
	30 °C	35 °C	
wild-type	++++	++++	
mot1–14	+++	+	W496ter, A614V, K626R
mot1–41	+++	+	L383P, Q412L, H444Q, F609L
mot1–42	+++	+	L383P
mot1–71	++++	+	L386S, Q404P, L446P, S467G, N595G, E680G, S685T
mot1–81	++++	+	L350S, T477A, L499P, I607P

[a] ++++, wild-type growth; fewer + signs indicate relatively slower growth.

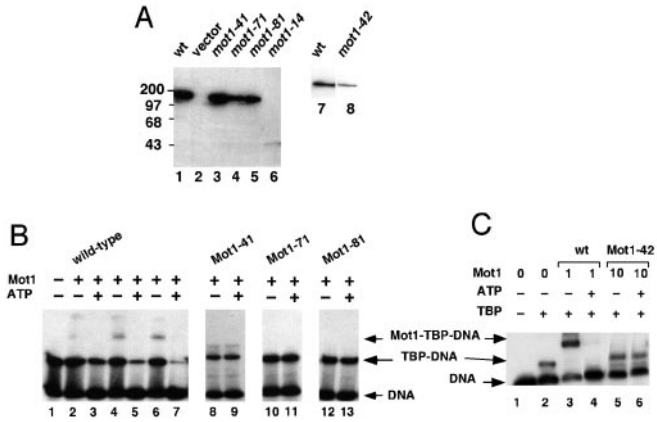

FIG. 2. **Analysis of temperature-sensitive *mot1* alleles.** *A*, Western blot (Py monoclonal antibody) analysis of Mot1 protein levels present in whole cell extracts prepared from strains carrying the indicated *mot1* allele. "*wt*" refers to wild-type Mot1. In extract from the strain labeled "*vector*," Mot1 is present but is untagged. In *lanes 1–6*, the indicated *mot1* alleles were expressed from the *GAL1* promoter. Similarly, in *lanes 7* and *8*, the level of wild-type Mot1 was compared with the level of Mot1-42. *B*, TBP and radiolabeled TATA-containing DNA were combined and wild-type or mutant Mot1 proteins were added subsequently in the presence or absence of ATP. The positions of the free DNA, TBP·DNA complex, and Mot1·TBP·DNA ternary complex are indicated by the *arrows*. DNA (0.5 nM) and TBP (5 nM) were present in all of the reactions. *Lanes 2–7* contained wild-type Mot1 as follows: reactions in *lanes 2* and *3* contained 0.75 nM Mot1, *lanes 4* and *5* contain 2.25 nM Mot1 and *lanes 6* and *7* contain 3.75 nM Mot1 (estimated by activity, see "Materials and Methods"). *Lanes 8–13* contained 2–3 units of the mot1 mutant proteins (based on concentration as determined by Western blotting). *C*, gel shift assay comparing activity of wild-type Mot1 to Mot1-42. Wild-type Mot1 was used at 10 nM in *lanes 3* and *4*, and Mot1-42 at 100 nM in *lanes 5* and *6*.

helical structure (22); thus, alanine scanning of polar residues should not affect the overall fold but could inhibit polar interactions. Mot1 missing the entire A block (Mot1-260; deletion of amino acids 1–98) does not support cell viability (Table II) even though this N-terminally truncated protein is expressed at wild-type levels (not shown). The A block is thus essential for Mot1 function *in vivo*. The Mot1-260 protein is also defective for formation of Mot1·TBP·DNA ternary complexes and ATP-dependent disruption of TBP·DNA *in vitro* (Fig. 3*A*, *lanes 3* and *4*). Similarly, deletion of the "linker" connecting A and B blocks generated a non-functional protein *in vivo* and *in vitro* (mot1–274; Fig. 3*A* and Table II) suggesting that important residues are located within the linker or that the A and B blocks must be appropriately positioned for Mot1 to function.

Site-directed A block mutant alleles were constructed on low copy plasmids under control of the *MOT1* or *GAL1* promoter and introduced into a yeast strain containing a deletion of the chromosomal copy of *MOT1*. All of the conserved charged and polar residues within the A block were mutated to alanine either singly or in clusters, and, remarkably, none of these residues were found to be essential for Mot1 function *in vivo*, even though many of these residues are conserved across species (see Fig. 1*B*, data are summarized in Table II). Strains carrying each of the *MOT1*-driven A block alleles were also screened for growth defects at 16 °C, 32 °C, and 35 °C but no ts or cold-sensitive phenotypes were observed (not shown). These strains also display no growth defects on synthetic or rich media with glucose, galactose, or raffinose as the carbon source (not shown).

In contrast to the normal growth observed with the A block alanine mutations when expressed under control of the *MOT1* promoter, several A block mutant alleles displayed a severe dominant-negative phenotype when expressed from the *GAL1* promoter. *GAL1*-driven *MOT1* is expressed at a 20–50-fold higher level than *MOT1* under control of the *MOT1* promoter (Fig. 3*B*, *lane 1 versus 2*). As summarized in Table II, *GAL1*-expressed alleles of *MOT1*-encoding mutations at the extreme N terminus severely inhibited cell growth when cells were grown on galactose in the presence of wild-type Mot1. The most severe defect was seen in *MOT1–101* cells (Table II). *MOT1–101* and wild-type *MOT1* were expressed at equivalent levels under *GAL1* control (Fig. 4*B*), and severe growth defects were observed on plates containing galactose or galactose plus raffinose (not shown), indicating that these alleles do not simply confer an inability of cells to metabolize galactose. In the absence of the wild-type *MOT1* gene, cells expressing *MOT1–101* were inviable on galactose-containing media, cells expressing *mot1-204*, *mot1-205*, or *mot1-206* grew more slowly than wild-type cells at 30 °C, and *mot1-204* and *mot1-205* conferred ts growth at 35 °C (not shown). The lethality induced by *GAL1*-driven *MOT1–101* is due to elevated expression levels of this protein, because cells grew well with *MOT1–101* as the sole source of Mot1 when the allele was expressed under control of the normal *MOT1* promoter (Table II).

Alleles of *MOT1* that encode proteins that recognize TBP but are defective in ATP-dependent TBP·DNA disruption exert dominant-negative effects on cell growth (41). This is due to interference with TBP function, because these dominant-negative phenotypes can be suppressed by overexpression of *SPT15*, which encodes TBP (41). To determine if the dominant-negative A block mutants interfere with TBP function *in vivo*, high copy plasmids expressing *SPT15* were introduced into strains expressing the dominant-negative A block allele *MOT1–101*. As shown in Fig. 3*C*, the lethality induced by *GAL1*-driven *MOT1–101* can be suppressed by *SPT15* overexpression. Side-by-side comparisons (not shown) demonstrate that overexpression of *SPT15* does not fully restore growth of these strains to wild-type rates, but these results suggest that the lethality induced by these A block mutations can be explained, at least in part, by interference with normal TBP function *in vivo*. *SPT15* overexpression was unable to suppress the growth defect in the *GAL1-MOT1–101* cells in which *MOT1–101* was the only source of Mot1 (not shown). This suggests that elevated levels of Spt15 suppress *MOT1–101* by interacting with the encoded mutant protein and thereby allowing wild-type Mot1 to function. As shown in Fig. 3*D*, Mot1-101 does recognize and dissociate TBP·DNA complexes *in vitro*, but the affinity of Mot1-101 for TBP·DNA complexes is reduced

TABLE II
Growth of strains harboring site-directed mutations in mot1

Allele	A-block mutations	*MOT1* promoter[a]	*GAL1* promoter
mot1–101	R7A, D9A, R10A	+++	−/dominant-negative
mot1–204	S3A, R4A, S6A	+++	++/weak dom. neg.[b]
mot1–205	R7A	+++	ts/dom. neg.
mot1–206	D9A	+++	ts/weak dom. neg.
mot1–207	R10A	+++	+++
mot1–211	R66A	+++	+++
mot1–212	H74A	+++	+++
mot1–213	N90A, E91A, S93A	+++	+++
mot1–215	E16A, T17A, S19A, T20A	+++	+++
mot1–216	R24A, N25A	+++	+++
mot1–217	D29A, Q30A, D33A	+++	+++
mot1–218	K36A, Q37A, H38A, E40A, D41A	+++	+++
mot1–219	S47A, R48A	+++	+++
mot1–236	S77A, D79A, N81A	+++	+++
mot1–237	E59A, T60A, R61A, T63A	+++	+++
mot1–238	K56A, K57A	+++	+++
mot1–241	E82A, S83A, D84A	+++	+++
Allele	B-block mutations	*MOT1* promoter	*GAL1* promoter
mot1–6	R501A, D503A, D504A, D505A	+++	+++
mot1–102	E308A, R310A, H311A	−	−
mot1–103	R318A, E319A, K322A	+++	+++
mot1–104	D361A, R362A, D365A	−	−
mot1–246	E308A	+++	+++
mot1–247	R310A	++	+++
mot1–248	H311A	+++	+++
mot1–252	R362A	+++	+++
mot1–253	D365A	−	−
mot1–261	D361A	−	−
Allele	Deletion	*MOT1* promoter	*GAL1* promoter
mot1–260	Δ1–98	−	−
mot1–274	Δ98–274	Not tested	−

[a] +++, wild-type growth; ++ or +, slower growth than cells with wild-type *MOT1;* −, no detectable single colonies.
[b] ts, temperature-sensitive growth at 35 °C; dom.neg., slow growth of cells harboring both wild-type *MOT1* and the mutant *mot1* allele.

at least 16-fold compared with wild-type Mot1. Possible molecular explanations for the growth defects of *MOT1–101* cells are discussed below.

Alanine Scanning Mutations in the MOT1 B Block—Mutations were also engineered in conserved clusters of charged or polar amino acids in the Mot1 B block (residues 289–583, Fig. 1*A*). The B block overlaps significantly with the region of the open reading frame mutagenized for the ts screen described above. Mutant alleles were expressed in yeast cells on low copy plasmids under control of the *MOT1* promoter or the *GAL1* promoter as for the A block mutants, and the results are summarized in Table II. Mutation of Glu-308, Arg-310, and His-311 resulted in a recessive loss-of-function allele (*mot1-102*; Table II). *mot1-102* is expressed at wild-type levels (Fig. 4*B*), and this protein does not detectably recognize or disrupt TBP·DNA complexes (Fig. 4*A*). Mutation of conserved residues Asp-361 or Asp-365 also results in complete loss of Mot1 function *in vivo* (Table II). The Mot1-104 protein, which contains both of these amino acid changes is expressed at wild-type levels (Fig. 4*B*), and, like Mot1-102, does not detectably bind or disrupt TBP·DNA complexes *in vitro* (Fig. 4*A*). Two alleles with wild-type *in vivo* function that encode changes in highly conserved residues were analyzed biochemically and found to recognize TBP·DNA complexes and support ATP-dependent TBP·DNA disruption equivalently to wild-type Mot1 (Mot1-103 in Fig. 4*A*, Mot1-216 in 4*C*). Thus, the ability of the *MOT1* alleles to support growth and the abilities of the encoded proteins to support TBP·DNA disruption are correlated.

TBP Residues That Participate in Mot1 Binary and Ternary Complex Formation—The Mot1·TBP binary complex binds DNA poorly (13). This suggests either that Mot1 interacts with the DNA-binding surface of TBP or that Mot1 induces a conformational change in TBP that affects the ability of TBP to bind to DNA. These results also suggest that Mot1 contacts TBP differently depending on whether TBP is bound to DNA. The N terminus of a human Mot1 homolog, BTAF1, also binds to TBP and can inhibit TBP binding to DNA (21). To better define how Mot1 recognizes TBP, TBP mutants were tested *in vitro* for the ability to interact with Mot1 in the absence of DNA. TBP mutants that retain DNA binding activity were also tested to determine if Mot1 could catalyze disruption of their interaction with DNA. Mot1 was loaded onto antibody-coupled beads as previously described (20), the beads were incubated with full-length TBP and washed, and the TBP association with the beads was assayed by Western blotting using TBP antibodies. TBP was retained on beads loaded with Mot1, whereas TBP binding to beads alone was nearly undetectable (Fig. 5*A*, *lanes 5* and *9 versus lane 3*). Control experiments established that the Mot1·TBP binary interaction was insensitive to ethidium bromide and DNase I, indicating that the association was not mediated by contaminating DNA (Fig. 5*A*, *lanes 5 versus 7* and *9 versus 11*). Because Mot1 used in these experiments was obtained from a yeast overexpression system, we also established that there was no contaminating TBP in the affinity-purified Mot1 preparation, and the TBP retained by the Mot1 beads therefore resulted from the interaction of Mot1 with the recombinant TBP added to the reactions (Fig. 5*A*, *lanes 12–15*).

Two mutants with solvent-exposed amino acid changes in the same α helix (helix 2) on the "top" convex surface of TBP were tested for interaction with Mot1 in this assay. As shown in Fig. 5*B*, TBP K138L and K145L were both defective for interaction with Mot1. TBP Lys-145 was previously shown to be critical for Mot1 recognition of TBP·DNA complexes (38), and TBP K133L,K138L was shown to be defective for Mot1-catalyzed disruption (12). TBP K138L·DNA complexes are not sta-

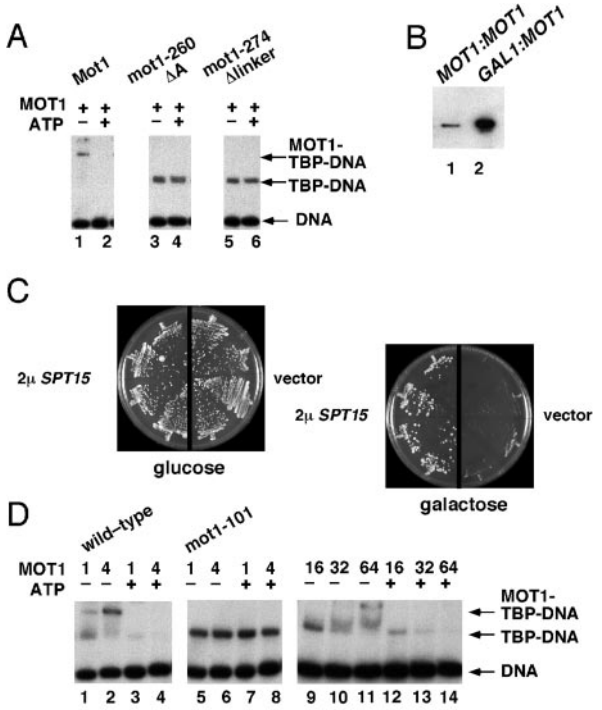

FIG. 3. **Mutational analysis of the Mot1 A block.** *A*, gel mobility shift analysis of purified wild-type Mot1 (*lanes 1* and *2*) *versus* mot1 derivatives missing the entire A block (residues 1–98; *lanes 3* and *4*) or missing residues between the A and B blocks (98–274; *lanes 5* and *6*). Core domain TBP was used at 5 nM, Mot1 and derivatives at 10 nM, and the DNA concentration was 0.5 nM. The abundance of the TBP·DNA complex was unaffected by addition of 3–10-fold more of either mot1 derivative (not shown). ATP (5 μM) was added where indicated. *B*, the levels of Mot1 protein expressed from the *MOT1* promoter *versus* the *GAL1* promoter were compared by Western blotting. The levels of Mot1 were 20–50-fold higher in cells with *MOT1* under *GAL1* control than when the *MOT1* gene was under *MOT1* promoter control. *C*, suppression of the *GAL1-MOT1–101* dominant-negative growth defect by overexpression of *SPT15*, the gene encoding TBP. Yeast strain YPH499 (33) was transformed with a *CEN ARS* plasmid containing *GAL1-MOT1–101* and a 2-μm vector carrying *SPT15* or the 2-μm vector without *SPT15* ("*vector*"). Four independent transformants from each transformation were re-streaked to glucose-containing plates (*left panel*) or galactose-containing plates (*right panel*). On the glucose-containing plate, the *GAL1*-driven *MOT1–101* gene is not expressed, and all strains grew equivalently; on galactose, *GAL1-MOT1–101* expression inhibited cell growth (*right panel*), but this defect is suppressed by overexpression of *SPT15* (*right panel*). 2-μm *SPT15* alone does not affect cell growth on glucose- or galactose-containing media (Ref. 41 and data not shown). *D*, gel mobility shift analysis as in Fig. 2 (*B* and *C*) using wild-type Mot1 (*lanes 1–4*) or Mot1-101 (*lanes 5–14*) plus or minus ATP as indicated. The relative amounts of Mot1 or Mot1-101 added are indicated. 1 unit of Mot1 (~5 nM, see "Materials and Methods") shifts a fraction of the TBP·DNA complex to the Mot1·TBP·DNA ternary complex (*lane 1*) and nearly completely disrupts TBP·DNA in the presence of ATP (*lane 3*). In contrast, 64-fold more Mot1-101 is required to obtain ternary complex formation similar to 1 unit of wild-type Mot1 (*lane 11*); ~32-fold more Mot1-101 is required to disrupt TBP·DNA complexes to the extent seen with 1 unit of wild-type Mot1 (*lane 13*).

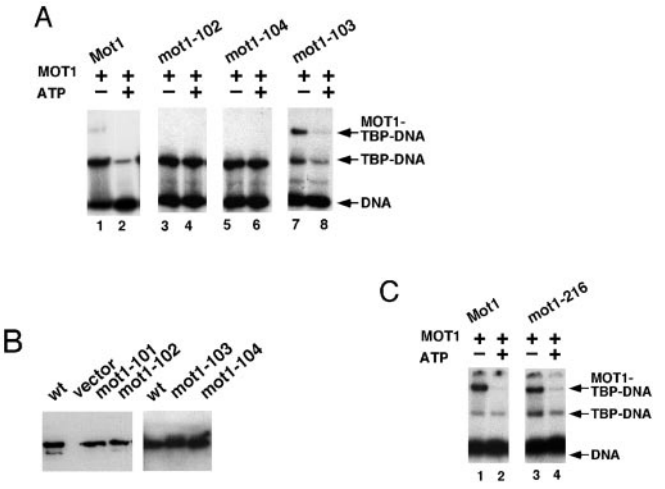

FIG. 4. **Mutational analysis of the Mot1 B block.** *A*, gel mobility shift analysis was performed using purified wild-type Mot1, mot1–102, mot1–103, or mot1–104 as indicated, with TBP and radiolabeled DNA (as in Fig. 2*B*). Ten micromolar ATP was added as indicated. Mot1 (or mutants) was present at about 5 nM. Titrations of Mot1 proteins demonstrated that Mot1-103 functions as well as wild-type Mot1 in this assay, whereas Mot1-102 and Mot1-104 have no detectable TBP·DNA binding or disruption activity. Reactions in *lanes 3–6* contained about 2-fold more Mot1 protein (judged by Western blotting) than the amount of wild-type Mot1 protein required for full activity in this assay. *B*, Western analysis (Py monoclonal antibody) of whole cell extracts prepared from cells containing the indicated *GAL1*-driven alleles of *MOT1*. Cultures of cells were grown to mid-log in raffinose-containing medium then induced with the addition of galactose to 2% for 2 h prior to harvest. "*Vector*" refers to extract from cells harboring plasmid with no epitope-tagged *MOT1* gene. *C*, gel mobility shift analysis as in *A* using purified Mot1-216, which displays ternary complex formation and TBP·DNA disruption activity equivalent to wild-type Mot1.

bly bound Mot1 (Fig. 5*D*), demonstrating that mutation of either Lys-138 or Lys-145 alone is sufficient to block recognition by Mot1. Thus, these residues on the convex surface of TBP are required for interaction with Mot1 in both the presence and absence of DNA. TBP Lys-127 is located at the extreme N terminus of helix 2 near the upstream edge of the TBP DNA-binding surface (see Fig. 9*A*). Whereas TBP K127L is defective for interaction with Mot1 in the absence of DNA (Fig. 5*B*), Mot1 can stabilize the interaction of TBP K127L with DNA to some extent, and the Mot1·TBP K127L·DNA ternary complex dissociates in the presence of ATP (Fig. 5*E*). This residue may define a difference in the architecture of the Mot1·TBP and Mot1·TBP·DNA complexes, or alternatively, this ternary complex may fall apart during ATP hydrolysis simply because TBP K127L binds DNA poorly.

Three TBPs with mutations on the DNA-binding surface were also tested for interaction with Mot1. As shown in Fig. 5*B*, TBP N159D retained the ability to interact with Mot1, whereas TBP V71E and TBP V161E do not interact detectably with Mot1 in this assay. The Mot1 N terminus binds weakly to TBP·DNA (20), and the Mot1 N terminus is also sufficient for formation of the Mot1·TBP binary complex (Fig. 5*C*). As was observed with the full-length Mot1 protein, there was no detectable binding of the Mot1 N terminus to TBPs with mutations in critical residues on the convex (K145L) or concave, DNA binding (V71E) surface of TBP. These results are consistent with and extend previously published results (21) and suggest that the inability of Mot1·TBP complexes to bind to DNA (13) is due to a direct interaction between Mot1 and the TBP binding surface. Remarkably, this would imply that the Mot1 N terminus embraces TBP via an extensive surface, making specific contacts with TBP simultaneously on opposite sides of the molecule.

Conformational Change of Mot1·TBP Binary Complex Induced by ATP—The Mot1·TBP binary complex does not detectably bind DNA *in vitro*, but it does hydrolyze ATP (20). Addition of ATP to pre-formed Mot1·TBP complexes allows TBP·DNA complexes to assemble on a DNA template that is too short to support Mot1-catalyzed disruption (13). One interpretation of these results is that Mot1 dissociates from TBP in the presence of ATP. Other experimental approaches have led to the conclusion that ATP does not induce the Mot1·TBP complex to dissociate (15), suggesting that disruption of Mot1·TBP binary complexes requires both ATP and DNA. To test this idea,

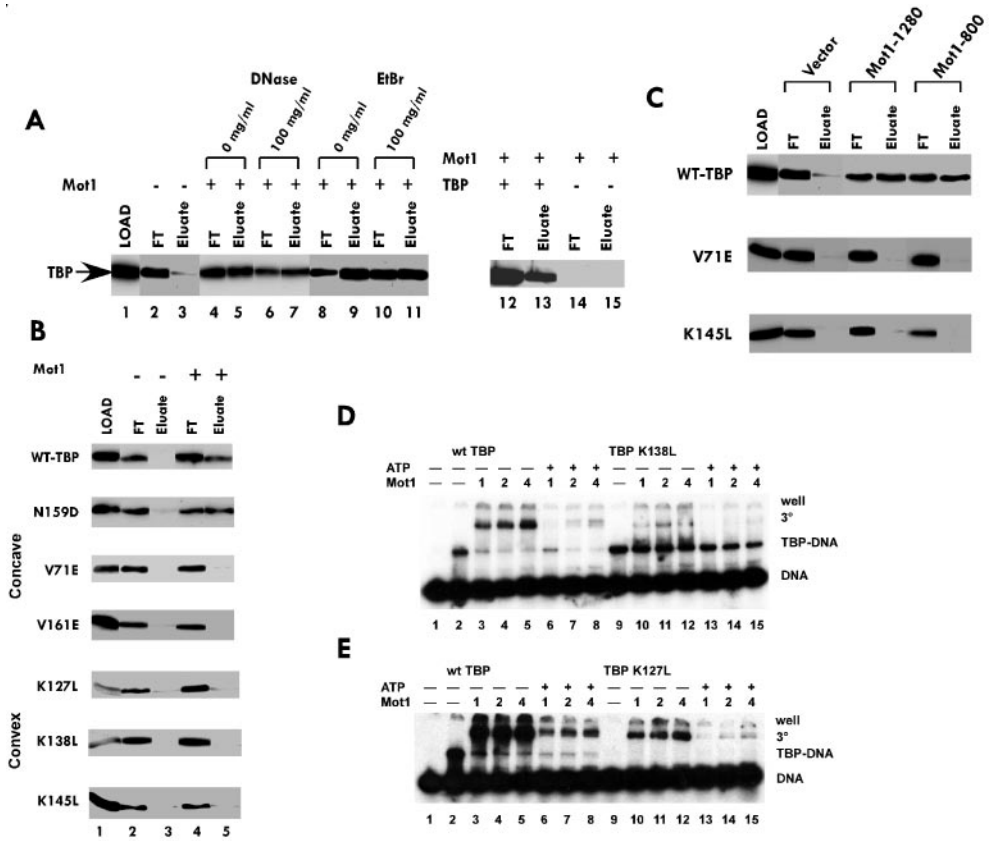

FIG. 5. **TBP DNA-binding surface is critical for Mot1 binding to TBP.** *A*, TBP interaction with Mot1 bound to agarose beads. Agarose beads with or without Mot1 (as indicated) were incubated with recombinant full-length TBP. The unbound flow-through (*FT*) and bead-bound materials (*Eluate*) were analyzed by Western blotting using a rabbit polyclonal antibody directed against TBP. DNase I or ethidium bromide (*EtBr*) were included in the wash buffers as indicated. In the reaction analyzed in *lanes 14* and *15*, no recombinant TBP was added; the absence of detectable TBP signal indicates that TBP did not contaminate the Mot1 preparation used for these studies. *B*, interaction of recombinant TBP or TBP mutants with agarose beads or Mot1 beads. The analysis was performed as in *A* using wild-type TBP or mutants as indicated. Note that wild-type TBP and TBP N159D are the only proteins that bound detectably to Mot1 beads (*lane 5*). *C*, binding of wild-type TBP or TBP mutants to beads alone (*vector*) or Mot1 N-terminal fragments bound to beads. Mot1-1280 is a Mot1 fragment with residues 1–1280, and Mot1-800 has the first 800 residues of Mot1 (see Fig. 1*A*). Analysis was performed as in *A* and *B* of this figure. *D*, gel mobility shift analysis was performed using radiolabeled DNA, Mot1, and the indicated TBPs as in Fig. 2*C*. *Lane 1* shows position of free DNA. *Lanes 2–8* each contain 2.5 nM purified recombinant full-length wild-type TBP. *Lanes 9–15* each contain 2.5 nM purified recombinant TBP K138L. Relative amounts of purified Mot1 were added as indicated, where 1 unit (*lane 3*) is ~5 nM. Note that TBP K138L·DNA complexes are unaffected by Mot1. *E*, gel mobility shift analysis as in *D* but using TBP K127L where indicated. *Lane 1* shows position of free DNA. Reactions in *lanes 2–8* each contained 2.5 nM purified recombinant full-length wild-type TBP, and reactions in *lanes 9–15* each contained 25 nM purified recombinant TBP K127L (a longer exposure is shown than in *panel D*). Relative amounts of purified Mot1 were added as in *D*. TBP K127L is defective for DNA binding, and the TBP K127L·DNA complex was barely detectable under these conditions. However, Mot1 stabilized TBP K127L binding to DNA (note ternary complex in *lanes 10–12*), and the complex dissociated in the presence of ATP (*lanes 13–15*).

three different experimental approaches were compared directly. In the first experiment, ATP and a 17-bp TATA DNA sequence (too short to support Mot1 binding, see "Materials and Methods" and Ref. 13) were added to a reaction containing the pre-formed Mot1·TBP binary complex. As shown in Fig. 6*A* (*lanes 7* and *8*), ATP induced the dissociation of Mot1·TBP binary complexes and formation of TBP·DNA complexes when a short DNA template was added to the reaction. Using a standard 36-bp DNA template that does support Mot1 action (Fig. 6*A*, *lanes 1–6*), Mot1 can load onto pre-formed TBP·DNA complexes and disrupt them using ATP, but, as expected, no TBP·DNA complexes were detected when the DNA and ATP were added to Mot1·TBP complexes, because any TBP loaded onto this DNA template was dissociated by Mot1. Consistent with these and previously published results (15), Mot1 bound to GST-TBP beads was not released in the presence of ATP alone (Fig. 6*B*). In contrast, however, ATP and DNA catalyzed release of less than half the Mot1 from GST-TBP beads (Fig. 6*B*, *lane 5*). The simplest interpretation of these results is that ATP and DNA can induce dissociation of the Mot1·TBP binary complex, but that tethering TBP to agarose beads impairs the catalytic activity of Mot1. Similar results were obtained in a reciprocal experiment using Mot1 bound to agarose beads and TBP in solution (not shown).

To better define the effect of ATP on the Mot1·TBP binary complex, a non-denaturing gel electrophoresis assay was used, but TBP and Mot1 were monitored by Western blotting rather than using radiolabeled DNA as in a conventional gel shift experiment. Under these conditions, free TBP was positively charged and entered a gel run toward the negative electrode (37). As shown in Fig. 6*C* (*lanes 1–6*), addition of Mot1 diminished the amount of free TBP that entered the gel. Mot1 was also incubated with TBP K138L, a TBP mutant that is not recognized by Mot1 (see Fig. 5). As shown in Fig. 6*C* (*lanes 9–14*), the amount of free TBP K138L was not diminished by addition of Mot1 so the decrease in the amount of TBP detected when Mot1 was added is not trivially due to degradation of TBP. Although TBP is slightly positively charged, Mot1 is predicted to have a slight negative charge under these conditions and the bulky Mot1·TBP binary complex is apparently nearly uncharged and did not enter gels run toward either the positive or the negative electrode. The negatively charged

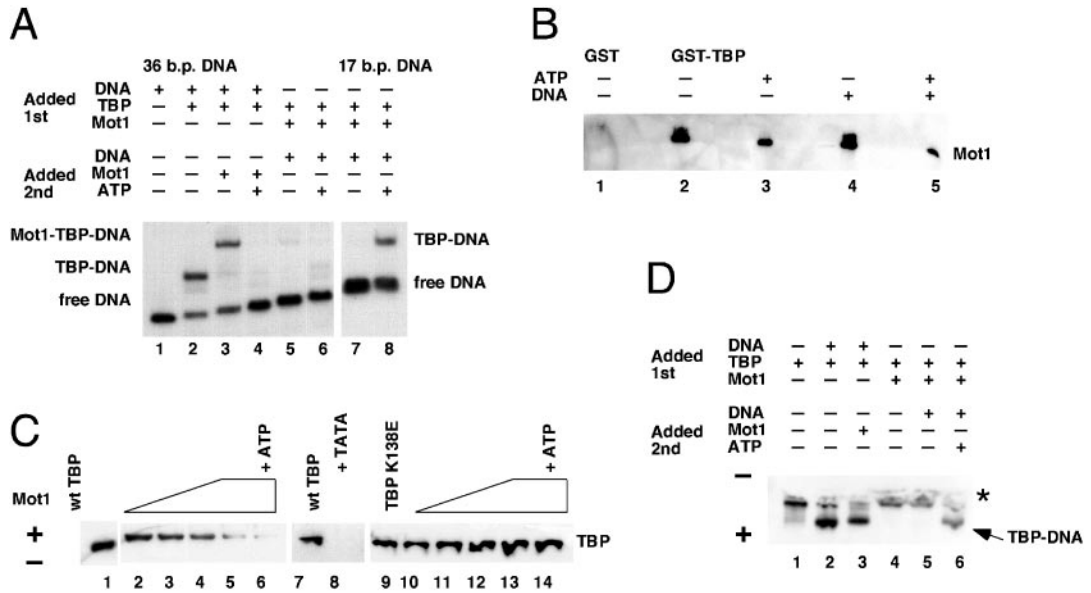

FIG. 6. **DNA and ATP together facilitate Mot1·TBP dissociation.** *A*, gel mobility shift assay using radiolabeled TATA-containing DNAs of different lengths. 5 nM TBP, 0.5 nM DNA, 5 μM ATP, and 40 nM Mot1 were added where indicated. Positions of free DNA, TBP·DNA, and Mot1·TBP·DNA ternary complex are shown. TBP core domain was incubated with either Mot1 or DNA for 30 min then either loaded on the gel or incubated with DNA or Mot1 with or without ATP for 30 min before loading. The order in which components were incubated for each reaction is shown *above the lanes*. Reactions were loaded at 2-min intervals, accounting for the gradual upward trend of the free DNA and TBP·DNA bands as the reactions were loaded from *left* to *right*. Mobility of the TBP·DNA complex is affected by DNA length (not shown). *B*, bead-bound Mot1·TBP complexes were incubated with ATP and/or DNA (as indicated), and the beads were washed to remove unbound material. The beads were then boiled in SDS sample buffer, and the bead-bound material was analyzed for Mot1 by Western blotting using the Py monoclonal antibody (see "Materials and Methods"). Reaction in *lane 1* was performed with GST beads, whereas reactions in *lanes 2–5* were performed using GST-TBP. Note that no detectable Mot1 bound to GST-Sepharose beads (*lane 1*), whereas ATP and DNA caused less than half of the bound Mot1 to be dissociated from GST-TBP beads (*lane 2 versus lane 5*). *C*, TBP alone (*lane 1*) or full-length TBP plus Mot1 (*lanes 2–7*) were incubated in the absence (*lanes 1–6*) or presence (*lane 7*) of ATP. An identical series of reactions were run in parallel using TBP K138L rather than wild-type TBP (*lanes 9–14*). The reactions were loaded at the top onto non-denaturing polyacrylamide gels and electrophoresed with electrodes connected as shown. Following electrophoresis, Western analysis was performed to detect TBP or TBP K138L. The *band* represents monomeric TBP (37). The reaction in *lane 1* contained no Mot1, 2.5 nM Mot1 was used in the reaction in *lane 2*, 10 nM Mot1 in *lane 3*, 30 nM Mot1 in *lane 4*, and 80 nM Mot1 in *lanes 5–6*. *Lane 10* contains 5 nM Mot1, and the Mot1 concentration doubles in each of the next three lanes to 40 nM in *lanes 13–14*. *D*, the experiment was performed as in *C* except that the gel was run with the electrodes reversed, to visualize negatively charged species. The position of the TBP·DNA complex is shown. The *asterisk* indicates a TBP-containing species (likely an aggregated form of TBP) that is present in the TBP preparation but does not affect the interpretation of the results.

TBP·DNA complex could be detected, however (Fig. 6*D*, *lane 2*). As expected, the Mot1·TBP·DNA ternary complex was not formed on the 17-bp DNA used (Fig. 6*D*, *lane 3*). Importantly, addition of ATP to Mot1·TBP binary complexes did not result in release of free TBP (Fig. 6*C*, *lane 6 versus 5*). However, addition of ATP and DNA to pre-formed Mot1·TBP complexes resulted in the appearance of the TBP·DNA complex (Fig. 6*D*, *lane 6*), consistent with the results in Fig. 6*A*. We conclude that while the Mot1·TBP binary complex hydrolyzes ATP, addition of ATP alone does not induce the complex to fall apart. However, the Mot1·TBP binary complex can be dissociated in a reaction that contains both ATP and DNA. Mot1·TBP complexes bound to agarose beads do not support Mot1 catalytic activity.

A Transition State ATP Analog Facilitates Loading of Mot1·TBP Complexes onto DNA—Because ATP does not induce Mot1·TBP binary complex dissociation but does facilitate TBP binding to DNA, we considered the possibility that locking the Mot1 ATPase into a conformational state somewhere along the catalytic path could generate a Mot1·TBP binary complex with enhanced DNA binding activity. This was tested using ADP aluminum fluoride (ADP-AlF_4), which binds to ATP-binding sites and mimics the presumed transition state of ATP during hydrolysis (39). ADP-AlF_4 does not cause disruption of the Mot1·TBP·DNA ternary complex (Fig. 7*A*, *lane 5 versus 3*), although ADP-AlF_4 appears to bind to the Mot1 ATP-binding site, because preincubation of Mot1 with ADP-AlF_4 prevents Mot1 from utilizing ATP added subsequently (Fig. 7*A*, *lanes 11–14*). Disruption of TBP·DNA complexes by Mot1 therefore requires ATP hydrolysis or perhaps multiple rounds of ATP hydrolysis. Consistent with the results in Fig. 6*A*, little Mot1·TBP·DNA ternary complex was detected when Mot1 and TBP were preincubated prior to addition of DNA (Fig. 7*A*, *lanes 6 versus 3*). However, addition of ADP-AlF_4 to pre-formed Mot1·TBP binary complexes allowed the binary complexes to load onto DNA (Fig. 7*A*, *lanes 8 versus 3* and *6*). Interestingly, addition of ADP-AlF_4 does not cause the Mot1·TBP binary complex to dissociate (Fig. 7*B*), suggesting that the Mot1·TBP·ADP-AlF_4 complex does not require interactions between Mot1 and the DNA-binding surface of TBP for stability or that Mot1 modulates the DNA binding activity of TBP exclusively by directing conformational changes in TBP. Thus, ADP-AlF_4 can convert the conformation of the Mot1·TBP binary complex into a form capable of binding DNA. Because ATP hydrolysis does not cause the binary complex to dissociate, these results support the hypothesis that one stage of the Mot1 ATP hydrolysis cycle opens or activates the binary complex to DNA binding.

Interaction of Mot1 with NC2·TBP·DNA—Because mutations on the DNA-binding surface of TBP impair interaction with Mot1, and ATP or ADP-AlF_4 can cause the TBP DNA-binding surface in the binary complex to become accessible to DNA, one simple model is that a portion of the Mot1 N terminus contacts the TBP DNA-binding surface and this interaction is transiently disrupted during the ATP hydrolysis cycle. NC2 specifically recognizes the "underside" of the TBP·DNA complex (42), so NC2 might block loading of or catalysis by Mot1 by prevent-

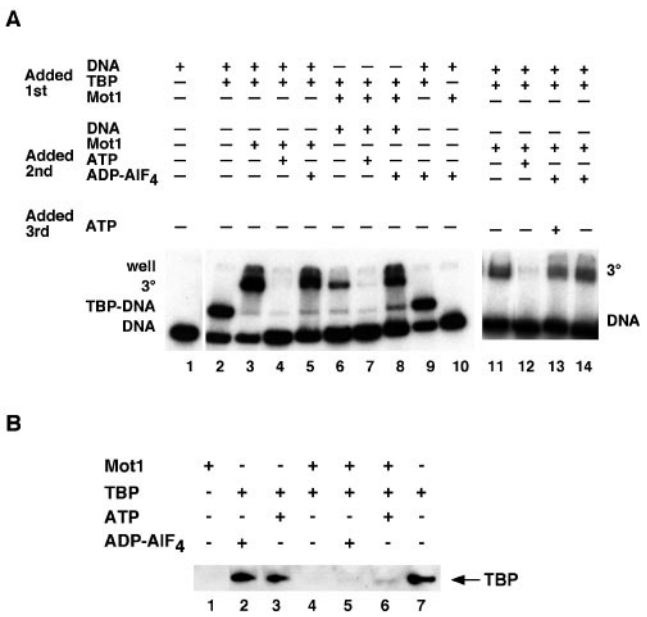

FIG. 7. **ATP transition state analog facilitates binding of Mot1·TBP complex to DNA.** *A*, gel mobility shift assay using radiolabeled 0.5 nM TATA DNA and 5 nM TBP. Approximately 40 nM Mot1, 5 μM ATP, and ADP-AlF_4 (see "Materials and Methods") were added where indicated. Orders of addition of DNA, TBP, Mot1, ATP, and ADP-AlF_4 are indicated. In the first incubation ("*Added 1st*"), components were incubated for 30 min. Additional components were then added as indicated ("*Added 2nd*"), and the reactions were incubated for 30 min and loaded onto the gel. ATP was added 10 min after $AlCl_3$ in *lane 13*. The position of the Mot1·TBP·DNA ternary complex is marked "*3°*." Phosphorimaging analysis showed that the ternary complex band in *lane 6* obtained after preincubation of Mot1 and TBP is only 10% the intensity of the ternary complex band in *lane 3*. The ternary complex bands in *lanes 5* and *8* are both 50% the intensity of the ternary complex band in *lane 3*, indicating 50% loss of the ternary complex in the presence of ADP-AlF_4, but that ADP-AlF_4 completely restores the ability of pre-formed Mot1·TBP complexes to bind to DNA. *B*, Mot1 alone (*lane 1*), TBP alone (*lanes 2*, *3*, and *7*) or TBP plus Mot1 (*lanes 4–6*) were incubated in the absence (*lanes 1*, *4*, and *7*) or presence of ATP (*lanes 3* and *6*) or ADP-AlF_4 (*lanes 2* and *5*). Proteins were incubated with ATP or ADP-AlF_4 for a total of 30 min. In reactions with both Mot1 and TBP, Mot1 was incubated with ATP or ADP-AlF_4 for 20 min, followed by addition of TBP for 10 min. The reactions were loaded onto non-denaturing polyacrylamide gels and electrophoresed as in Fig. 6*C*. Following electrophoresis, Western analysis was performed to detect TBP. The position of TBP is shown. Mot1 and TBP were used at 50 nM, ATP was 100 μM, and ADP-AlF_4 was used as described under "Materials and Methods."

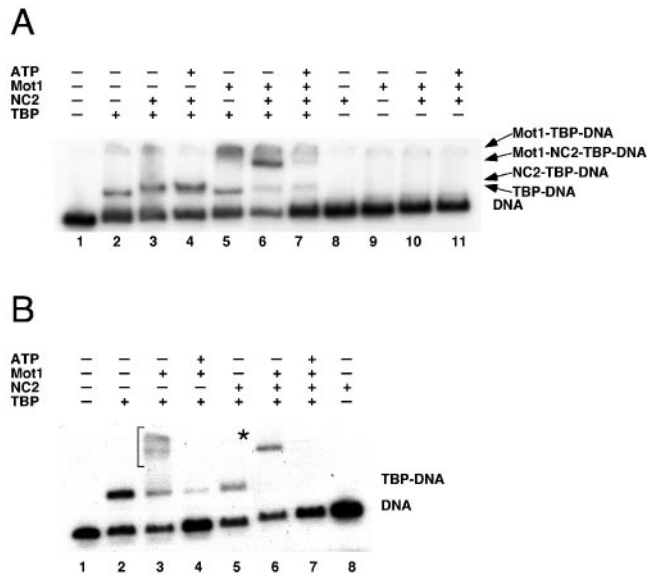

FIG. 8. **Mot1 binds and disrupts the TBP·NC2·DNA complex.** *A*, gel mobility shift analysis using a Tris borate-EDTA (*TBE*) native gel, 0.5 nM radiolabeled TATA DNA, and 5 nM TBP. The positions of the various complexes are indicated by the *arrows*. Mot1 (5 nM) and NC2 (composed of Bur6, 13 nM, and Ydr1/Ncb2, 60 nM) were added where indicated. *B*, gel mobility shift analysis using a Tris-glycine (*TG*) native gel was performed using radiolabeled TATA DNA, TBP, Mot1, and NC2 as in *A*. The *bracket* in *lane 3* marks the Mot1·TBP·DNA shift, which was not discrete in this experiment. The *asterisk* indicates the distinct Mot1·NC2·TBP·DNA shift.

ing Mot1 from interacting with the concave surface of TBP. There is also a striking overlap of the gene sets whose transcription is controlled by NC2 and Mot1, suggesting a mechanistic interplay between them at specific promoters (11, 43–45). To address the biochemical interplay of Mot1 and NC2 *in vitro*, gel mobility shift experiments were performed. The gel mobility shifts of the Mot1·TBP·DNA and NC2·TBP·DNA complexes were readily distinguished with the NC2·TBP·DNA complex migrating just slightly more slowly than the TBP·DNA complex (Fig. 8*A*). Addition of both Mot1 and NC2 resulted in the appearance of a new species (Fig. 8*A*, *lane 6*). The same results were observed in both TBE gels (Fig. 8*A*), which favor the NC2·TBP·DNA shift, and in TG gels (Fig. 8*B*, compare band marked by the *bracket* with that marked by the *asterisk*), which stabilize the TBP·DNA shift but destabilize the NC2·TBP·DNA shift. These results show that Mot1 and NC2 do not compete for TBP binding; rather, they cooperate to form Mot1·NC2·TBP·DNA quaternary complexes. In addition, ATP caused disruption of the quaternary complex (Fig. 8*A*, *lane 6 versus 7*; Fig. 8*B*, *lane 6 versus 7*), indicating that NC2 also provides no barrier to Mot1-catalyzed TBP·DNA disruption.

DISCUSSION

Mot1 is an essential, conserved yeast protein (7) that interacts genetically and biochemically with TBP (14, 41). Mot1 catalysis of TBP·DNA disruption can explain its role as a repressor of transcription (43), but how Mot1 activates transcription and the mechanism of the TBP·DNA disruption reaction are unknown. The results in this paper provide mechanistic insight into how the Mot1 ATPase is used to drive TBP·DNA disruption *in vitro*, and *in vivo* analysis of Mot1 mutants demonstrates a close correlation between the ability of Mot1 to catalyze TBP·DNA disruption and the ability to provide the essential function of Mot1 *in vivo*. These results also explain previous data demonstrating inhibition of TBP DNA binding by Mot1. Furthermore, the role of ATP in opening the Mot1·TBP binary complex to DNA binding suggests a model, discussed below, for how Mot1 catalyzes TBP·DNA disruption.

Leucine Repeats in the Mot1 N Terminus—The leucine repeats of the Mot1 N-terminal domain have been identified as either HEAT (24) or ARM (22) repeats. In either case, the leucine repeats of Mot1 coincide with the blocks of conserved sequence in the N terminus (Fig. 1). There is no structural information about them, but these results suggest that the Mot1 N terminus probably adopts an extended conformation, similar to importin β (46, 47) or β catenin (48). The Mot1 N terminus is sufficient for TBP binding (Fig. 5*C*) and is necessary for activation of the ATPase (20). Karyopherin 114, an importin β family member, binds TBP (49, 50), so there may be other TBP-hydrophobic repeat interactions.

A direct test of the ARM/HEAT repeat model for Mot1 is not possible because of the limited structural information on Mot1 and the large size of the Mot1 N terminus. Hydrophobic residues are also predicted to play important roles in both stabilization of interactions between leucine repeats and interaction with TBP, but Mot1 proteins with mutations in hydrophobic residues would also be expected to be defective, because mutation of residues in the hydrophobic core of the protein could

lead to instability of the native structure. A deeper understanding of the structural basis of the Mot1 defects reported here awaits future structural analysis.

Function of the Mot1 A Block—The A block is required for the Mot1·TBP interaction (Fig. 3*A*), yet most of the conserved polar residues of the A block can be changed to alanines without affecting cell viability (Table II). Only the mutation of a few of the first ten amino acids of the protein had any effect. In particular, mutation of Arg-7, Asp-9, and Arg-10 caused dominant inhibition of cell growth when the mutant gene was expressed from the *GAL1* promoter (*MOT1–101*), and *GAL1*-controlled alleles encoding mutations in Arg-7 or Asp-9 conferred temperature-sensitive growth. Overexpression of *SPT15* rescued cells from overexpression of *MOT1–101* (Fig. 3*C*), supporting the idea that the dominant negativity is due to an altered interaction with TBP. Mot1-101 protein is defective for binding TBP·DNA but has no obvious catalytic defect (Fig. 3*D*). One possibility is that the Mot1-101·TBP binary complex may be unusually stable: recycling of TBP after Mot1 action may be required *in vivo*. Formation of Mot1-101·TBP binary complexes could not be assessed *in vitro* using the pull-down assay, because purified Mot1-101 was found to interact nonspecifically with agarose beads (not shown), perhaps suggesting that the N terminus of Mot1-101 is not stably folded. Alternatively, the polar residues at the Mot1 N terminus may be important for an interaction with another protein that modulates the catalytic activity of Mot1 *in vivo*.

Two Putative Mot1-binding Sites on TBP—Previous results (19, 38) and those in Fig. 5 demonstrate that the interaction of Mot1 with TBP requires lysine residues in TBP helix 2, on the convex surface of TBP opposite the DNA-binding site (Fig. 9*A*). These residues are required for both binary and ternary complex formation. A second putative Mot1-binding site is located on the concave DNA-binding surface of TBP and is defined by valine 71 and valine 161 (Fig. 9*A*). Mutation of these residues disrupts interaction with both DNA and Mot1, but these altered TBP molecules are unlikely to be simply misfolded, because they are expressed in soluble form at normal levels (not shown) and these same TBPs can stimulate transcription *in vivo* (51). A direct interaction between the DNA-binding surfaces of Mot1 and TBP can explain why the Mot1·TBP binary complex does not bind DNA. Interestingly, although Mot1 does not form a binary complex with TBP K127L, Mot1·TBP K127L·DNA ternary complexes were detectable, and these ternary complexes were disrupted in the presence of ATP (Fig. 5, *B* and *E*). Similarly, a TBP with altered specificity for DNA binding supports Mot1·TBP·DNA ternary complex formation and ATP-dependent disruption (30) but is defective for binary interaction with BTAF1, a human Mot1 homolog (21). We suggest that Mot1 contacts the convex surface of TBP in both binary and ternary complexes and that Mot1 interaction with TBP alone requires a direct interaction between Mot1 and the TBP DNA-binding surface. In contrast, Mot1 does not directly interact with the TBP DNA-binding surface in Mot1·TBP·DNA ternary complex, but instead contacts the DNA upstream of the TATA box (13). Recent data (52) demonstrate that human TBP Lys-138 can affect DNA binding despite being located on the opposite side of the TBP DNA-binding surface. Therefore, an alternative possibility is that the effects of TBP DNA-binding surface mutations on Mot1 interaction result from reciprocal changes in TBP conformation rather than a direct interaction with Mot1. This possibility remains to be tested.

ATP Switches Mot1·TBP Binary Complex Affinity for DNA—The inability of Mot1·TBP binary complexes to bind DNA can be overcome by addition of ATP and the use of a DNA probe that is too short to allow Mot1 binding (13). We interpreted this result to indicate that the binary complex dissociates in the presence of ATP. On the other hand, an immobilized binary complex does not dissociate in the presence of ATP (19), suggesting that both DNA and ATP are required for dissociation. Here we report that ATP hydrolysis by the binary complex does not cause the binary complex to dissociate but, rather, that ATP induces a change in Mot1·TBP conformation that allows TBP to bind to DNA and Mot1 to be released. Experiments with the non-hydrolyzable ATP analog ADP-AlF_4 provided additional support for this model. Although binding of ADP-AlF_4 by Mot1 is not sufficient to drive Mot1·TBP·DNA ternary complex dissociation, ADP-AlF_4 did allow the binary complex to load onto DNA (Fig. 7*A*).

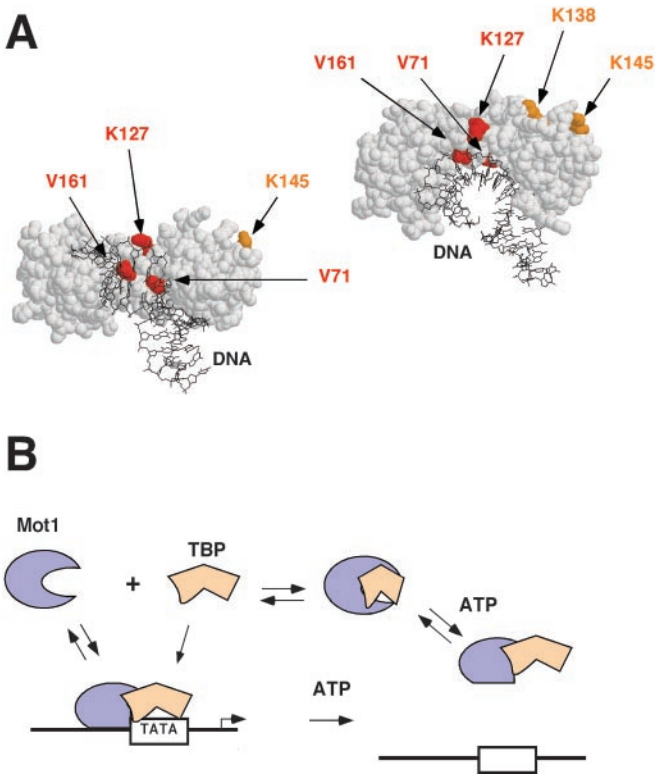

FIG. 9. **Model for Mot1 catalytic cycle and the role of ATP.** *A*, *S. cerevisiae* TBP·DNA structure (56). Residues required for Mot1·TBP binary complex formation are shown in *red*. Residues required for Mot1·TBP·DNA ternary complex formation are shown in *orange*. DNA is *black*. *B*, Mot1 binds TBP·DNA reversibly via interaction with the convex surface of TBP and upstream DNA. The data support a model in which the Mot1·TBP complex is stabilized by interactions between Mot1 and both the convex and concave surfaces of TBP, and the binary complex does not readily dissociate or bind DNA. An alternative possibility that is consistent with the data is that Mot1 binding induces a conformational change in TBP (shown as a distorted TBP in the Mot1·TBP binary complex), and the altered conformation of TBP binds DNA poorly. At one step in the ATP hydrolysis cycle, mimicked by binding of ADP-AlF_4, the Mot1·TBP complex has an altered conformation in which the DNA-binding surface of TBP is either transiently accessible to DNA or TBP assumes its high affinity DNA binding conformation. ATP hydrolysis induces dissociation of the Mot1·TBP binary complex from DNA by weakening interaction of TBP with DNA, possibly through formation of contacts between Mot1 and the TBP DNA-binding surface.

Mechanism of Disruption—Several mechanisms have been proposed for protein·DNA disruption by the Snf2/Swi2-related ATPases, including Mot1 (13, 28, 53, 54). In contrast to mechanisms employed by at least some chromatin remodeling enzymes, Mot1 does not use ATP hydrolysis to propagate DNA bending, twisting, or strand separation through the TATA box (13). Mot1 also does not use ATP hydrolysis to track processively along DNA (30). Mot1-mediated changes in TBP confor-

mation have been proposed to explain how Mot1 regulates the interaction between TBP and DNA (15). In support of the TBP conformational change model, human TBP·K138 modulates DNA binding affinity (52), a result suggesting that amino acids distal to the DNA-binding surface can affect DNA binding by directing a change in TBP conformation. Because this residue is critical for the interaction of yeast TBP and Mot1 (Fig. 5), it is possible that Mot1 interaction with the convex surface of TBP causes a change in the conformation of the TBP DNA-binding surface that is modulated by ATP.

The effects of TBP DNA-binding surface mutations on Mot1 interaction are most simply explained, however, by proposing a direct interaction between Mot1 and the DNA-binding surface of TBP. Combining this with previous observations, we propose the mechanism shown in Fig. 9*B*. The catalytic cycle then involves an ATP-driven insertion of the Mot1 N terminus into the TBP·DNA interface. This "power stroke" results in disruption of TBP·DNA contacts and the formation of new interactions between Mot1 and the DNA-binding surface of TBP. Once separated from DNA, the binary complex can hydrolyze ATP in a process that involves dramatic conformational changes in which the Mot1 N terminus alternates position in and out of contact with the DNA-binding surface of TBP. The conformation in which the DNA-binding surface of TBP is "open" can be trapped with ADP-AlF_4, a state in which TATA-containing DNA can bind to TBP. Note that in the model (Fig. 9*B*), the conformation of TBP is different in the Mot1·TBP binary complex than when TBP is free, reflecting the possibility that Mot1 may induce a conformational change in TBP as part of its catalytic mechanism.

Mechanistic Insights Provided by Mot1-NC2 Interaction—Chromatin immunoprecipitation experiments established that both Mot1 and the NC2 subunit Bur6 are localized to the promoters that they regulate (43, 55). Microarray experiments have shown that Mot1 and Bur6 regulate many of the same genes (43, 45). The results in Fig. 8 demonstrate that Mot1 and NC2 can occupy the same promoter at the same time and show that NC2 does not impede the catalytic activity of Mot1. Thus, if such catalytic activity is altered at some promoters, as has been suggested to explain how Mot1 can activate the expression of some genes (43), this putative change in biochemical activity must depend on promoter-associated factors other than the NC2 complex. In addition, because Mot1 does not interfere with access of NC2 to TBP·DNA, Mot1 is unlikely to contact the underside of the TBP·DNA complex and the catalytic action of Mot1 is unlikely to require contact with the major groove of the TATA box.

Acknowledgments—We are grateful to Kai Post for construction of the *MOT1* mutant plasmid library, Ron Reeder for the GST-TBP expression plasmid, Bob Roeder, Frank Pugh, and Tetsuro Kokubo for yeast TBP expression plasmids, and Greg Prelich for TBP K145E and the purified NC2 components. We are also grateful to Tatsuya Hirano for communicating results prior to publication, to Tony Weil for advice on the non-denaturing gel-electrophoretic analysis of protein·protein complexes, and to Dan Engel, Patrick Grant, Tsuyoshi Miyake, and members of the Auble laboratory for comments on the manuscript.

REFERENCES

1. Kotani, T., Banno, K., Ikura, M., Hinnebusch, A. G., Nakatani, Y., Kawaichi, M., and Kokubo, T. (2000) *Proc. Natl. Acad. Sci. U. S. A.* **97,** 7178–7183
2. Struhl, K. (1999) *Cell* **98,** 1–4
3. Maldonado, E., Hampsey, M., and Reinberg, D. (1999) *Cell* **99,** 455–458
4. Pugh, B. F. (2000) *Gene* (*Amst.*) **255,** 1–14
5. Berk, A. J. (1999) *Curr. Opin. Cell Biol.* **11,** 330–335
6. Lee, T. I., and Young, R. A. (1998) *Genes Dev.* **12,** 1398–1408
7. Davis, J. L., Kunisawa, R., and Thorner, J. (1992) *Mol. Cell. Biol.* **12,** 1879–1892
8. Jiang, H., Xie, Y., Houston, P., Stemke-Hale, K., Mortensen, U. H., Rothstein, R., and Kodadek, T. (1996) *J. Biol. Chem.* **271,** 33181–33186
9. Karnitz, L., Morrison, M., and Young, E. T. (1992) *Genetics* **132,** 351–359
10. Piatti, S., Tazzi, R., Pizzagalli, A., Plevani, P., and Lucchini, G. (1992) *Chromosoma* **102,** S107–S113
11. Prelich, G. (1997) *Mol. Cell. Biol.* **17,** 2057–2065
12. Auble, D. T., and Hahn, S. (1993) *Genes Dev.* **7,** 844–856
13. Darst, R. P., Wang, D., and Auble, D. T. (2001) *EMBO J.* **20,** 2028–2040
14. Poon, D., Campbell, A. M., Bai, Y., and Weil, P. A. (1994) *J. Biol. Chem.* **269,** 23135–23140
15. Adamkewicz, J. I., Mueller, C. G., Hansen, K. E., Prud'homme, W. A., and Thorner, J. (2000) *J. Biol. Chem.* **275,** 21158–21168
16. van der Knaap, J. A., Borst, J. W., van der Vliet, P. C., Gentz, R., and Timmers, H. T. (1997) *Proc. Natl. Acad. Sci. U. S. A.* **94,** 11827–11832
17. Chicca, J. J., 2nd, Auble, D. T., and Pugh, B. F. (1998) *Mol. Cell. Biol.* **18,** 1701–1710
18. Goldman-Levi, R., Miller, C., Bogoch, J., and Zak, N. B. (1996) *Nucleic Acids Res.* **24,** 3121–3128
19. Adamkewicz, J. I., Hansen, K. E., Prud'homme, W. A., Davis, J. L., and Thorner, J. (2001) *J. Biol. Chem.* **276,** 11883–11894
20. Auble, D. T., Wang, D., Post, K. W., and Hahn, S. (1997) *Mol. Cell. Biol.* **17,** 4842–4851
21. Pereira, L. A., van der Knaap, J. A., van den Boom, V., van den Heuvel, F. A., and Timmers, H. T. (2001) *Mol. Cell. Biol.* **21,** 7523–7534
22. Andrade, M. A., Petosa, C., O'Donoghue, S. I., Muller, C. W., and Bork, P. (2001) *J. Mol. Biol.* **309,** 1–18
23. Andrade, M. A., Ponting, C. P., Gibson, T. J., and Bork, P. (2000) *J. Mol. Biol.* **298,** 521–537
24. Neuwald, A. F., and Hirano, T. (2000) *Genome Res.* **10,** 1445–1452
25. Gorbalenya, A. E., and Koonin, E. V. (1993) *Curr. Opin. Struct. Biol.* **3,** 419–429
26. Henikoff, S. (1993) *Trends Biochem. Sci.* **18,** 291–292
27. Eisen, J. A., Sweder, K. S., and Hanawalt, P. C. (1995) *Nucleic Acids Res.* **23,** 2715–2723
28. Havas, K., Flaus, A., Phelan, M., Kingston, R., Wade, P. A., Lilley, D. M., and Owen-Hughes, T. (2000) *Cell* **103,** 1133–1142
29. Cote, J., Peterson, C. L., and Workman, J. L. (1998) *Proc. Natl. Acad. Sci. U. S. A.* **95,** 4947–4952
30. Auble, D. T., and Steggerda, S. M. (1999) *Mol. Cell. Biol.* **19,** 412–423
31. Langst, G., and Becker, P. B. (2001) *Mol. Cell* **8,** 1085–1092
32. Leung, D. W., Chen, E., and Goeddel, D. V. (1989) *Technique* **1,** 11–15
33. Sikorski, R. S., and Hieter, P. (1989) *Genetics* **122,** 19–27
34. Guthrie, C., and Fink, G. R. (1991) *Guide to Yeast Genetics and Molecular Biology*, p. 194, Academic Press, Inc., San Diego
35. Schneider, K. R., Smith, R. L., and O'Shea, E. K. (1994) *Science* **266,** 122–126
36. Kim, T. K., and Roeder, R. G. (1997) *J. Biol. Chem.* **272,** 7540–7545
37. Banik, U., Beechem, J. M., Klebanow, E., Schroeder, S., and Weil, P. A. (2001) *J. Biol. Chem.* **276,** 49100–49109
38. Cang, Y., Auble, D. T., and Prelich, G. (1999) *EMBO J.* **18,** 6662–6671
39. Maruta, S., Henry, G. D., Sykes, B. D., and Ikebe, M. (1993) *J. Biol. Chem.* **268,** 7093–7100
40. Schuler, G. D., Altschul, S. F., and Lipman, D. J. (1991) *Proteins Struct. Funct. Genet.* **9,** 180–190
41. Auble, D. T., Hansen, K. E., Mueller, C. G., Lane, W. S., Thorner, J., and Hahn, S. (1994) *Genes Dev.* **8,** 1920–1934
42. Kamada, K., Shu, F., Chen, H., Malik, S., Stelzer, G., Roeder, R. G., Meisterernst, M., and Burley, S. K. (2001) *Cell* **106,** 71–81
43. Dasgupta, A., Darst, R. P., Martin, K. J., Afshari, C. A., and Auble, D. T. (2002) *Proc. Natl. Acad. Sci. U. S. A.* **99,** 2666–2671
44. Lemaire, M., Xie, J., Meisterernst, M., and Collart, M. A. (2000) *Mol. Microbiol.* **36,** 163–173
45. Andrau, J. C., Van Oevelen, C. J., Van Teeffelen, H. A., Weil, P. A., Holstege, F. C., and Timmers, H. T. (2002) *EMBO J.* **21,** 5173–5183
46. Cingolani, G., Petosa, C., Weis, K., and Muller, C. W. (1999) *Nature* **399,** 221–229
47. Vetter, I. R., Arndt, A., Kutay, U., Gorlich, D., and Wittinghofer, A. (1999) *Cell* **97,** 635–646
48. Huber, A. H., Nelson, W. J., and Weis, W. I. (1997) *Cell* **90,** 871–882
49. Morehouse, H., Buratowski, R. M., Silver, P. A., and Buratowski, S. (1999) *Proc. Natl. Acad. Sci. U. S. A.* **96,** 12542–12547
50. Pemberton, L. F., Rosenblum, J. S., and Blobel, G. (1999) *J. Cell Biol.* **145,** 1407–1417
51. Jackson-Fisher, A. J., Chitikila, C., Mitra, M., and Pugh, B. F. (1999) *Mol. Cell* **3,** 717–727
52. Zhao, X., and Herr, W. (2002) *Cell* **108,** 615–627
53. Gavin, I., Horn, P. J., and Peterson, C. L. (2001) *Mol. Cell* **7,** 97–104
54. Guyon, J. R., Narlikar, G. J., Sullivan, E. K., and Kingston, R. E. (2001) *Mol. Cell. Biol.* **21,** 1132–1144
55. Geisberg, J. V., Holstege, F. C., Young, R. A., and Struhl, K. (2001) *Mol. Cell. Biol.* **21,** 2736–2742
56. Kim, Y., Geiger, J. H., Hahn, S., and Sigler, P. B. (1993) *Nature* **365,** 512–520